Molecular Cancer Therapeutics

Sphingosine Kinase-1 Protects Multiple Myeloma from Apoptosis Driven by Cancer-Specific Inhibition of RTKs

Shuntaro Tsukamoto[1], Yuhui Huang[1], Motofumi Kumazoe[1], Connie Lesnick[2], Shuhei Yamada[1], Naoki Ueda[1], Takashi Suzuki[1], Shuya Yamashita[1], Yoon Hee Kim[1], Yoshinori Fujimura[3], Daisuke Miura[3], Neil E. Kay[2], Tait D. Shanafelt[2], and Hirofumi Tachibana[1,3,4]

Abstract

Activation of acid sphingomyelinase (ASM) leads to ceramide accumulation and induces apoptotic cell death in cancer cells. In the present study, we demonstrate that the activation of ASM by targeting cancer-overexpressed 67-kDa laminin receptors (67LR) induces lipid raft disruption and inhibits receptor tyrosine kinase (RTK) activation in multiple myeloma cells. Sphingosine kinase 1 (SphK1), a negative regulator of ceramide accumulation with antiapoptotic effects, was markedly elevated in multiple myeloma cells. The silencing of SphK1 potentiated the apoptotic effects of the green tea polyphenol epigallocatechin-3-*O*-gallate (EGCG), an activator of ASM through 67LR. Furthermore, the SphK1 inhibitor safingol synergistically sensitized EGCG-induced proapoptotic cell death and tumor suppression in multiple myeloma cells by promoting the prevention of RTK phosphorylation and activation of death-associated protein kinase 1 (DAPK1). We propose that targeting 67LR/ASM and SphK1 may represent a novel therapeutic strategy against multiple myeloma. *Mol Cancer Ther; 14(10); 2303–12. ©2015 AACR.*

Introduction

Multiple myeloma is the second most common hematologic malignancy. It is an incurable disease with an average survival of 5 years following high-dose chemotherapy and autologous stem cell transplantation or treatment with novel drugs such as lenalidomide and bortezomib (1). The 67-kDa laminin receptor (67LR) is overexpressed in various cancers, including multiple myeloma (2), acute myeloid leukemia (AML; ref. 3), colorectal carcinoma (4), and breast carcinoma (5). Pathologic studies suggest that increased 67LR expression is correlated with lesions histologic severity and tumor progression (4). Furthermore, 67LR overexpression in cancer has also been linked with increased expression levels of cyclins A and B and cyclin-dependent kinases (CDK)-1 and -2, whereas a mouse 67LR-knockdown model exhibited markedly reduced tumor growth (6). In addition, the overexpression of 67LR can also induce adhesion-mediated drug resistance and chemotherapy resistance (7). Therefore, these findings support a vital role for 67LR in cancer progression.

The green tea polyphenol epigallocatechin-3-*O*-gallate (EGCG) inhibits tumor cell growth and induces apoptosis in cancer cells without adversely affecting normal cells (2, 3, 8). Several clinical trials have been conducted to evaluate its potential role in cancer treatment (9–11). 67LR has been identified as a cell surface EGCG receptor that mediates an antitumor effect of EGCG *in vivo* (12, 13). Furthermore, 67LR is required for EGCG-induced selective killing of multiple myeloma and AML cells, whereas peripheral blood mononuclear cells (PBMC) are spared (2, 3). Such findings provide a rationale for the clinical evaluation of EGCG as a 67LR-targeting drug. However, the concentrations of EGCG required to achieve sufficient killing of multiple myeloma cells are much higher than the plasma concentrations achieved in clinical trials till date. Therefore, we focused on the key mediator of 67LR-dependent apoptotic cell death and amplified it using a molecular targeting strategy.

Insulin-like growth factor 1 receptor (IGF1R) regulates the proliferation, survival, and metastasis of many cancer cells, including multiple myeloma cells. Recent studies have shown that targeting IGF1R has impressive anticancer activity in both *in vitro* and *in vivo* models of breast, prostate, and colon cancers (14). EGCG has been proven as a potent inhibitor of IGF1R in colon cancer cells (15). However, the influence of EGCG on IGF1R activity in multiple myeloma cells remains unknown.

Acid sphingomyelinase (ASM) acts on membrane sphingomyelin to generate ceramide, which mediates cell death induced by diverse stimuli, such as ionizing radiation, chemotherapeutic agents and ultraviolet A (UVA) light (16). In addition, ASM-induced generation of ceramide leads to displacement of cholesterol from lipid rafts on the plasma membrane (17). However, whether ASM influences cholesterol-rich lipid raft formation, which is associated with receptor tyrosine kinase (RTK) activation (18), is unknown. We have previously reported the mechanisms by which protein kinase C (PKC) delta and ASM

[1]Division of Applied Biological Chemistry, Department of Bioscience and Biotechnology, Faculty of Agriculture, Kyushu University, Fukuoka, Japan. [2]Department of Medicine, Mayo Clinic, Rochester, Minnesota. [3]Innovation Center for Medical Redox Navigation, Kyushu University, Fukuoka, Japan. [4]Food Functional Design Research Center, Kyushu University, Fukuoka, Japan.

Note: Supplementary data for this article are available at Molecular Cancer Therapeutics Online (http://mct.aacrjournals.org/).

S. Tsukamoto and Y. Huang contributed equally to this article.

Corresponding Author: Hirofumi Tachibana, 6-10-1 Hakozaki, Higashi-ku, Fukuoka 812-8581, Japan. Phone: 81-92-642-3008; Fax: 81-92-642-3008; E-mail: tatibana@agr.kyushu-u.ac.jp

doi: 10.1158/1535-7163.MCT-15-0185

mediate EGCG-induced cell death via 67LR (19). However, whether 67LR/ASM signaling is involved in the inhibition of RTK activity remains unclear.

Sphingosine kinase 1 (SphK1) is overexpressed in multiple cancers, including those of the breast, prostate, ovary, and lung (20). SphK1 catalyzes the phosphorylation of sphingosine, promoting ceramide metabolism and formation of sphingosine-1-phosphate (S1P; ref. 21). S1P then activates G-protein–coupled receptors that control multiple cellular processes, including antiapoptosis, cell proliferation, and angiogenesis (21). Therefore, SphK1 regulates a rheostat, balancing the effects of proapoptotic ceramide and proproliferative S1P; and inhibiting SphK1 and downregulating S1P is a rational therapeutic target for cancer therapy (22). L-Threo-dihydrosphingosine (safingol) is a competitive inhibitor of SphK1, which first entered clinical trials as an anticancer agent. Unfortunately, safingol has limited single-agent activity *in vivo*, and strategies to increase its effectiveness in cancer treatment without increasing toxicity are urgently required (23).

We demonstrate that overexpression of SphK1 attenuates 67LR-dependent cancer cell death induced by EGCG. Our findings demonstrate that a novel combination of therapeutic agents (EGCG and safingol) shows potent synergistic toxicity in multiple myeloma cells, without affecting normal cells. The stimulation of ceramide generation by targeting 67LR and SphK1 is a simple and efficient strategy for myeloma-specific chemotherapy.

Materials and Methods

Materials and antibodies

EGCG, BODIPY-C12-sphingomyelin, catalase, and propidium iodide (PI) were purchased from Sigma. Annexin V–Alexa Fluor 488 and DiIC16 were obtained from Life Technologies Corporation. Safingol was purchased from Avanti Polar Lipids, Inc. Anti-ASM (H-181) and anti-phospho-EGFR (Y1173) antibodies were obtained from Santa Cruz Biotechnology; anti-67LR (MLuC5) and anti-SphK1 antibodies were purchased from Abcam. Anti-phospho-IGF1R (Y1131), anti-IGF1R, anti-EGFR, and anti-DAPK1 antibodies were purchased from Cell Signaling Technology. Anti-67LR serum was obtained from a rabbit, which had been immunized with synthesized peptides corresponding to residues 161 to 170 of human 67LR (24). Acid sphingomyelinase activity assay kit was obtained from Echelon Biosciences.

Patient samples and cell culture

Primary multiple myeloma cells were isolated from bone marrow aspirate samples obtained from patients with multiple myeloma. Patients provided informed consent and the studies were performed in accordance with the Declaration of Helsinki. The purity of plasma cells (80%) was confirmed by monitoring the cell surface expression of CD38 and CD138. Mononuclear cells were obtained from peripheral blood donated by 3 healthy volunteers who provided informed consent. U266, ARH-77, RPMI-8226 (a human multiple myeloma), and MPC-11 (a mouse myeloma) cell lines were purchased from ATCC between 2006 and 2007. Multiple myeloma patient cells, and all the cell lines were maintained in RPMI-1640 containing 10% FBS in a state of logarithmic growth at 37°C in humidified air with 5% CO_2. To assess *in vitro* experiment of EGCG, cells were plated in 24-well plates at 1×10^5 cells/mL and were treated with the indicated concentrations of EGCG for the indicated time period in RPMI-1640 supplemented with 1% FBS, 200 U/mL catalase, and 5 U/mL superoxide dismutase (SOD; Sigma). All cell lines used in the study were obtained.

Cell surface ceramide accumulation

After treatment with EGCG for 3 hours, cells were fixed with 2% paraformaldehyde. Cells were washed with PBS and blocked for 1 hour in 1% FBS/PBS. Cells were incubated with anti-ceramide antibody (1 mg/mL; Alexis) at 4°C for overnight, followed by incubation with secondary antibody (Alexa Fluor 488) for 30 minutes. Fluorescent images of cell surface ceramide were analyzed using a fluorescence microscope (Keyence; Photoshop Software, Adobe Systems; $n = 10$ per group).

LC-ESI-MS/MS analysis of ceramides

U266 cells were plated at 5×10^5 cells per sample and were treated with/without 20 μmol/L of EGCG for 2 hours with 5 μmol/L CAY10466 (Cayman Chemical). Cells were washed and transferred. Then, 25 pmol of each component of Ceamide/Sphingoid Internal Standard Mixture II provided by Avanti Polar Lipids was added as internal standard. After extracting lipids, 24 samples were redissolved with 20% mobile phase B in A solution (described below). A binary solvent gradient with a flow rate of 0.3 mL/min was used to separate sphingolipids by normal-phase chromatography using an InertSustain NH2 (GL Sciences). The chromatography was performed at 40°C and the gradient was started a 20% B (methanol/water/formic acid, 89/9/1, v/v/v, with 20 mmol/L ammonium formate) in A (acetonitrile/methanol/formic acid, 97/2/1, v/v/v, with 5 mmol/L ammonium formate) and reached 100% B in 4 minutes and maintained 100% B for 2 minutes. Finally, the gradient was returned to the starting conditions and the column was equilibrated for 5 minutes before the next run. Ceramide levels were determined by liquid chromatography–positive electrospray ionization/tandem mass spectrometry (LC-ESI-MS/MS) using a triple quadrupole mass spectrometer LCMS-8040 (Shimadzu Corporation). The detection was performed using multiple reaction monitoring (MRM) mode based on the specific ion transitions for ceramide molecular species as follows: m/z 482.5 > 264.2, 12:0-Cer; m/z 538.5 > 264.2, 16:0-Cer; m/z 566.6 > 264.2, 18:0-Cer; m/z 594.6 > 264.2, 20:0-Cer; m/z 622.6 > 264.2, 22:0-Cer; m/z 650.6 > 264.2, 24:0-Cer; m/z 648.6 > 264.2, 24:1-Cer (24). This analytic method was constructed according to previously reported articles (refs. 24, 25; $n = 4$ per group).

Western blotting

Immunoblot analysis was performed as previously described (26).

Lipid raft clustering assay

Cells were labeled with 750 nmol/L of DiIC16 labeling solution and then stimulated for varying times with EGCG. After treatment, cells were extracted with 0.5% Triton X-100 on ice for 30 minutes and then fixed with 2% paraformaldehyde. Fluorescent images of lipid raft staining were analyzed using a fluorescence microscope (Keyence; Photoshop Software, Adobe Systems; $n = 10$ per group).

In vitro cell proliferation and apoptosis assay

The number of cells was determined by trypan blue exclusion. Apoptotic multiple myeloma cells were detected using

Annexin V–Alexa Fluor 488 (Life Technologies Corporation). Cells were mixed with Annexin V–Alexa Fluor 488 and media-binding reagent, and a portion of the cell suspension was placed onto a glass slide and immediately observed under a fluorescence microscope, BZ-8100 (Keyence).

For flow cytometric analysis, the cells were double stained with Annexin V–Alexa Fluor 488 and propidium iodide (PI). The percentages of Annexin V^+ cells were calculated by combining Annexin V^+/PI^- (early Annexin V–positive) and Annexin V^+/PI^+ (late Annexin V–positive), followed by analysis using a FACSCalibur (Becton Dickinson and Company). A total of 1×10^4 cells were plated into 96-well plates and cultured in 1% FBS-RPMI containing the indicated concentrations of compounds in triplicate.

RTK activity assay

Cells were precultured in serum-free medium for 24 hours before being treated with the indicated compounds for 24 hours. After treatment, cells were stimulated with 10% FBS-RPMI for 30 minutes and analyzed for phospho-RTK expression levels using a phosho-RTK array kit (R&D Systems).

RNAi by shRNA

Lentiviral pLKO.1 vectors expressing nontargeting control shRNA or shRNAs targeting ASM (TRCN0000230097) and SphK1 (TRCN0000344943) were purchased from Sigma-Aldrich. Lentivirus production, transduction, and selection were performed according to the manufacturer's instructions.

Animals

BALB/c mice (Kyudo) were kept on a 12-hour light/12-hour dark cycle (light on at 8 am) in an air-conditioned room at 20°C and 60% humidity under specific pathogen-free conditions.

Multiple myeloma xenograft murine model

Five-week-old female BALB/c mice were inoculated subcutaneously in the interscapular area with 5×10^6 MPC-11 cells in 100 μL RPMI-1640 medium. Following the appearance of palpable tumors, mice were divided randomly into groups with an even distribution of tumor sizes (10 mice per group) and injected intraperitoneally daily with saline alone or EGCG (20 mg/kg) or safingol (5 mg/kg) every 2 days. Tumor growth was measured with calipers. Tumor volume was calculated as volume = length × width^2/2. Statistical analysis of survival curves was performed using log-rank analysis of Kaplan–Meier curves. This experiment was performed in accordance with law #105 and notification #6 of the Japanese government for the welfare of experimental animals. All procedures were approved by the Animal Care and Use Committee of Kyushu University and performed in strict accordance with institutional guidelines for handling laboratory animals.

Statistical analysis

Values for the *in vitro* studies represent the mean ± SD of at least 3 experiments. The significance of difference between the experimental variables was determined by Tukey test. Statistical analyses were performed using KyPlot software.

Results

Activated ASM induces lipid raft disruption

We used an ASM assay to identify a dose-dependent increase in ASM activity following treatment of multiple myeloma U266 cells with low concentrations of EGCG (Fig. 1A). In addition, microscopic (Fig. 1B) and LC-MS/MS (Fig. 1C) analyses revealed a dose-dependent increase in cell surface ceramide levels in U266 cells following EGCG treatment. Displacement of cholesterol from the lipid raft on the plasma membrane occurs after generation of ceramide by ASM (17), and EGCG has been shown to induce disruption of cholesterol-rich lipid rafts in colon cancer cells (27). Therefore, we next investigated the involvement of ASM in EGCG-induced disruption of lipid raft domains by staining with the lipid-mimetic dialkyl-indocarbocyanine (DilC16) and using a cold Triton X-100 solubility assay (Fig. 1D and E). Exposure of

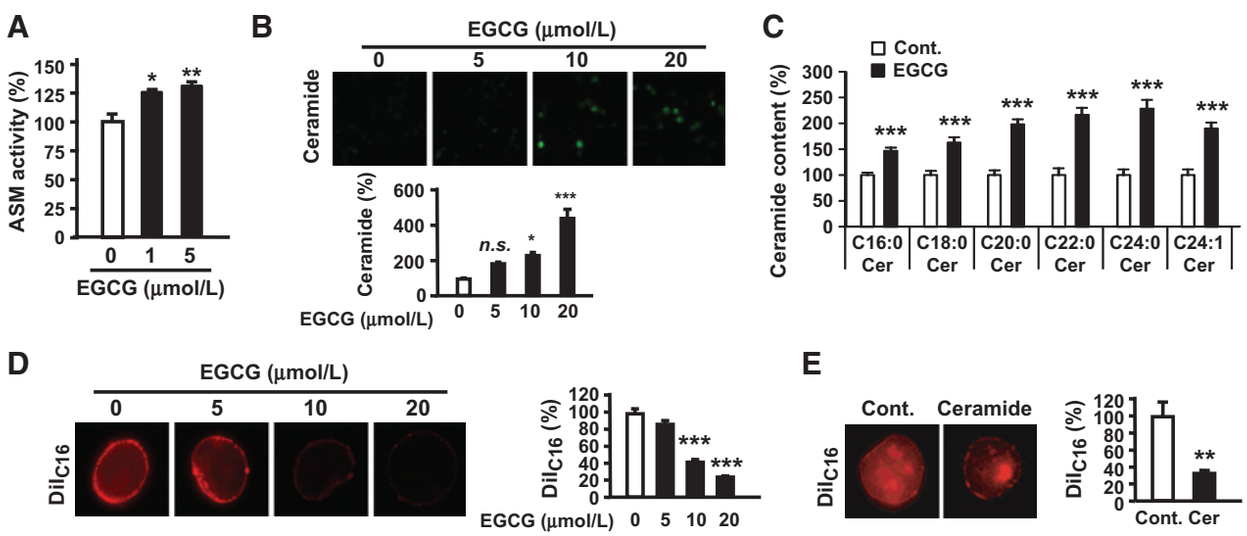

Figure 1.
Activated ASM induces lipid raft disruption. A, ASM activity following treatment with EGCG. B, cell surface ceramide levels after treatment with EGCG for 3 hours. C, LC-MS/MS analysis of ceramide levels after treatment with 20 μmol/L EGCG for 3 hours. D and E, U266 cells were stained with DilC16 and then exposed to EGCG (D) or C_{16}-ceramide (E) for 3 hours. Fluorescent images of lipid raft staining were analyzed using a fluorescence microscope. *, $P < 0.05$; **, $P < 0.01$; ***, $P < 0.001$; n.s., not significant.

myeloma U266 cells to C16-ceramide or EGCG (>10 μmol/L) caused a marked reduction in Triton X-100 resistance of the plasma membrane, indicating that EGCG-induced ceramide generation caused lipid raft disruption.

EGCG induces RTK inhibition via ASM activation

Previous studies have concluded that a cholesterol-rich lipid raft can function as a platform and is associated with RTK activation (18). We used a phospho-RTK array kit to determine the effect of EGCG on RTK activation. Treatment with 10 μmol/L EGCG inhibited FBS-induced phosphorylation of various RTKs, including EGF receptor (EGFR), v-erb-b2 erythroblastic leukemia viral oncogene homolog 2, neuro/glioblastoma-derived oncogene homolog (avian; ErbB2), v-erb-b2 erythroblastic leukemia viral oncogene homolog 3 (avian; ErbB3), IGF1R, c-mer proto-oncogene tyrosine kinase (Mer), hepatocyte growth factor (HGF) R, macrophage-stimulating protein (MSP) R, fms-related tyrosine kinase 3 (Flt-3), and macrophage colony-stimulating factor (M-CSF) R (Fig. 2A, Supplementary Fig. S1). However, EGCG had no influence on the phosphorylation level of most of the RTKs in ASM knockdown U266 cells (Fig. 2B and C). Moreover, pretreatment with anti-67LR antibodies blocked EGCG-induced

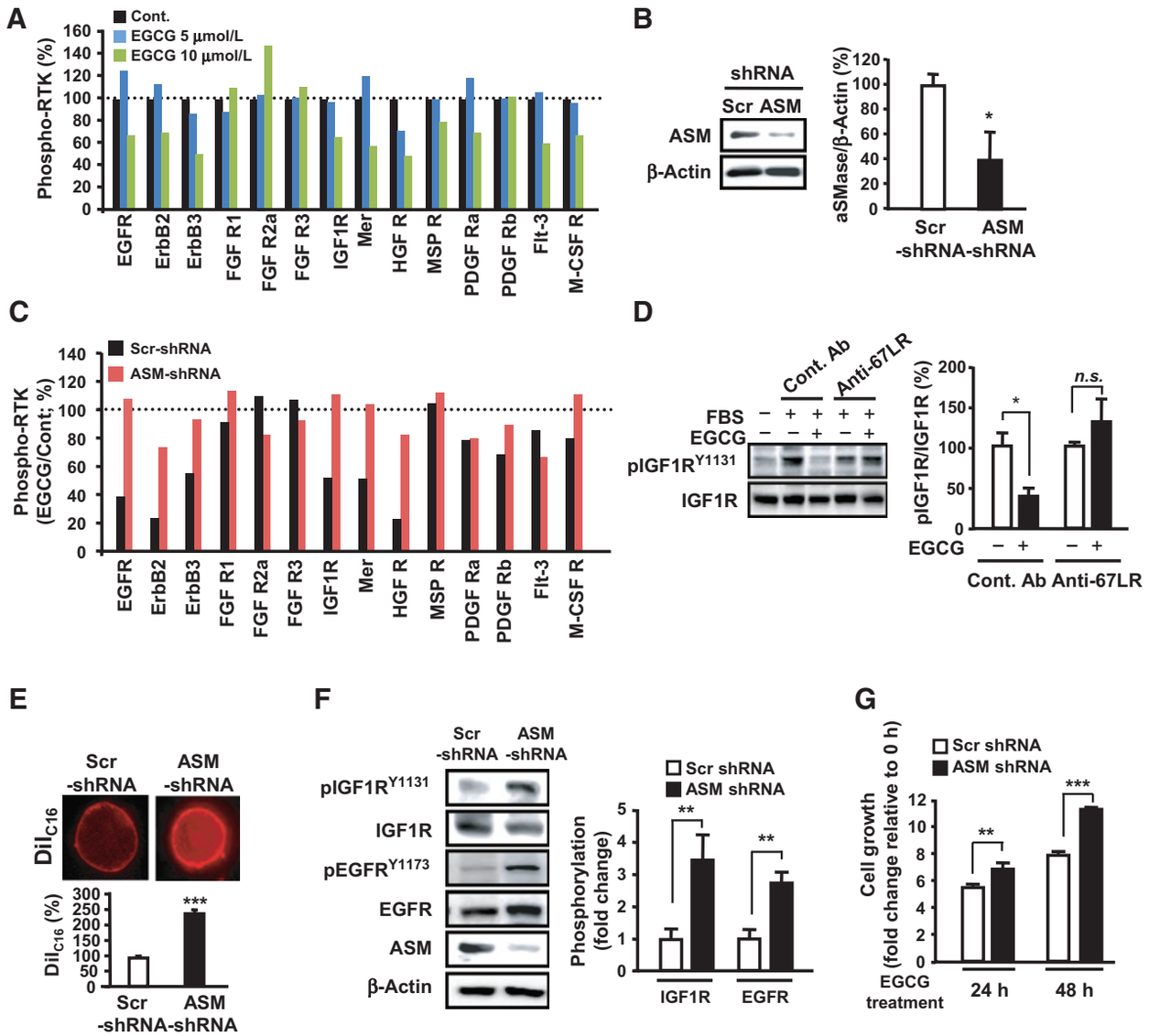

Figure 2.
EGCG induces RTK inhibition via ASM activation. A, effect of EGCG on the activities of multiple RTKs. B, shRNA-mediated knock down of ASM in U266 cells. C, effect of silencing ASM on EGCG-induced inhibition of RTKs in U266 cells. D, U266 cells were pretreated with either anti-67LR antibodies or control antibodies before stimulation with EGCG (10 μmol/L) for 24 hours, and IGF1R phosphorylation levels were detected by Western blot analysis. E, effect of silencing ASM on lipid raft clustering in U266 cells. Fluorescent images with lipid raft staining were analyzed using a fluorescence microscope in ASM-knocked down U266 cells. F, cells, precultured in serum-free medium for 24 hours, were stimulated with 10% FBS-RPMI for 30 minutes and analyzed for phospho-IGF1R and phospho-EGFR expression levels by Western blot analysis in ASM knocked down U266 cells. G, effect of silencing ASM on cell proliferation in U266 cells. Error bars, SD. $n = 3$ per group. *, $P < 0.05$; **, $P < 0.01$; ***, $P < 0.001$; n.s., not significant.

inhibition of IGF1R phosphorylation, suggesting that 67LR/ASM signaling mediates EGCG-induced inactivation of IGF1R (Fig. 2D).

Next, we performed cold Triton X-100 solubility assays and Western blot analysis on ASM-knockdown U266 cells to examine the effect of ASM on lipid raft localization and RTK activity (Fig. 2E–G). Transfection of U266 cells with an shRNA expression vector to reduce ASM expression increased cholesterol-rich lipid raft clustering and phosphorylation of IGF1R and EGFR and promoted cell growth. In addition, safingol potentiated EGCG-induced disruption of cholesterol-rich lipid rafts but did not have an effect on the clustering of ceramide-rich lipid rafts (Supplementary Fig. S2). Collectively, these results suggest that the 67LR/ASM pathway is necessary for EGCG-induced disruption of the lipid raft and inhibition of RTK phosphorylation in U266 cells.

Abnormal overexpression of SphK1 protects cells from EGCG-induced RTK inhibition

Our findings revealed that ASM-generated ceramide contributes to EGCG-induced anti-myeloma activity, suggesting that targeting negative regulators of ceramide could enhance sensitivity to EGCG. EGCG induced ASM activation at low concentrations (1 μmol/L), but did not stimulate ceramide accumulation or disruption of lipid raft formation unless cells were treated with more than 10 μmol/L EGCG. We hypothesized that SphK1 may protect cancer cells from EGCG-induced cell death by downregulating ceramide levels and upregulating S1P levels in multiple myeloma cells (Fig. 3A). We found that SphK1 levels were markedly increased in multiple myeloma cells isolated from patients and all human multiple myeloma cell lines, compared with normal PBMCs from healthy donors (Fig. 3B). To determine the impact of SphK1 on the EGCG-induced disruption of lipid rafts, cells were treated with EGCG and safingol, an SphK1 inhibitor. We observed significant disruption of the lipid raft and accumulation of ceramide following combination treatment of U266 cells with both EGCG and safingol (Fig. 3C and Supplementary Fig. S3A and S3B). In addition, FBS-induced RTK phosphorylation—including that of IGF1R—was suppressed following treatment of U266 cells with the EGCG/safingol combination (Fig. 3D and E).

SphK1 protects cells from 67LR/ASM-dependent apoptotic cell death induced by EGCG

To determine the impact of SphK1 on the anti–multiple myeloma activity of EGCG, cells were treated with EGCG and safingol. Safingol treatment potently increased EGCG-induced cell death in multiple myeloma cells isolated from patient samples and all multiple myeloma cell lines while having no observable harmful effect on normal PBMCs (Fig. 4A). This EGCG/safingol-induced specific cell death was attributed to apoptosis (Fig. 4B and C). Treatment with EGCG and safingol in combination resulted in greater inhibition of the growth of U266 cells, with an IC_{50} of 5.4 μmol/L compared with 28.3 μmol/L for EGCG alone (Supplemental Fig. S4A–S4C). Isobologram analyses showed that the growth-inhibitory effect of combined treatment with EGCG and safingol on the growth of U266 cells was synergistic (Supplementary Fig. S4D).

SphK2 is another isoform of SphK; therefore, we examined the effects of SphK2 on EGCG-induced cell death. Silencing the expression of SphK2 did not affect the EGCG-induced cell death

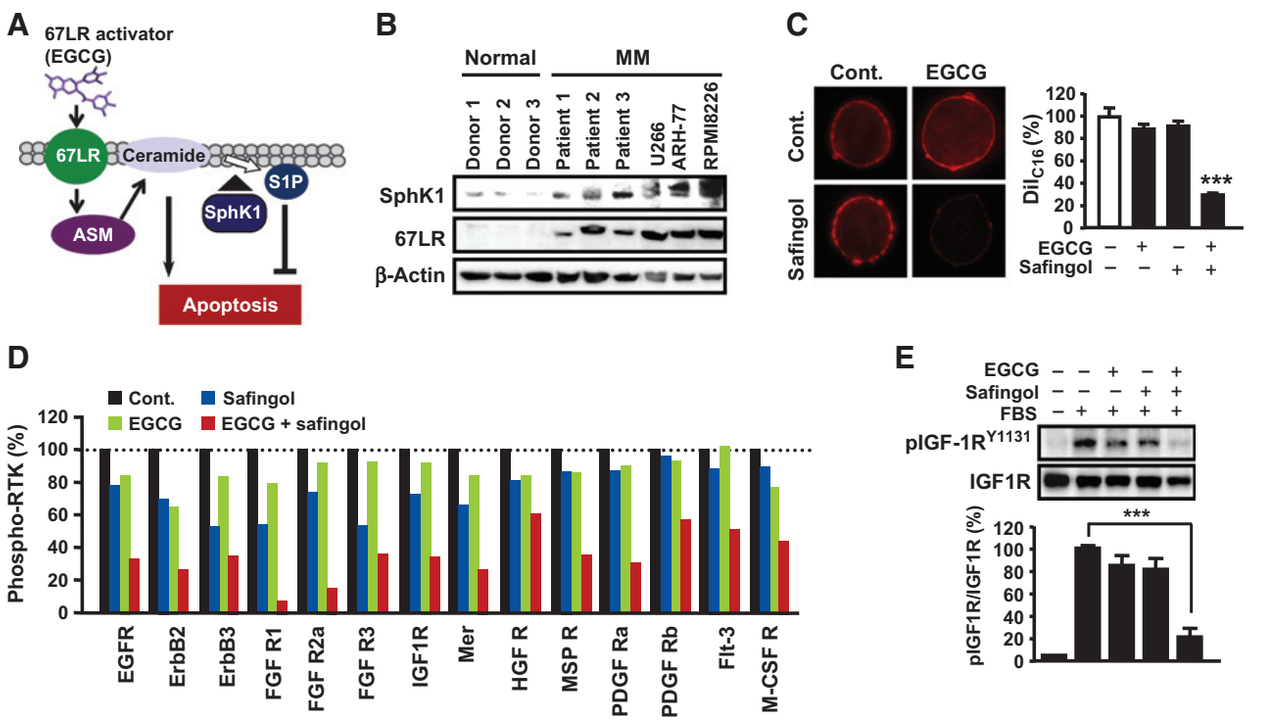

Figure 3.
Abnormal overexpression of SphK1 protects cells from EGCG-induced inhibition of RTKs. A, schematic of ceramide generation mediated by 67LR/ASM signaling and ceramide metabolism. B, 67LR and SphK1 expression levels in patient multiple myeloma cell lines and normal PBMCs. C, lipid raft clustering in U266 cells treated with 5 μmol/L EGCG/1 μmol/L safingol. D and E, effect of 5 μmol/L EGCG/1 μmol/L safingol on the activities of multiple RTKs (D) and IGF1R phosphorylation (E). ***, $P < 0.001$.

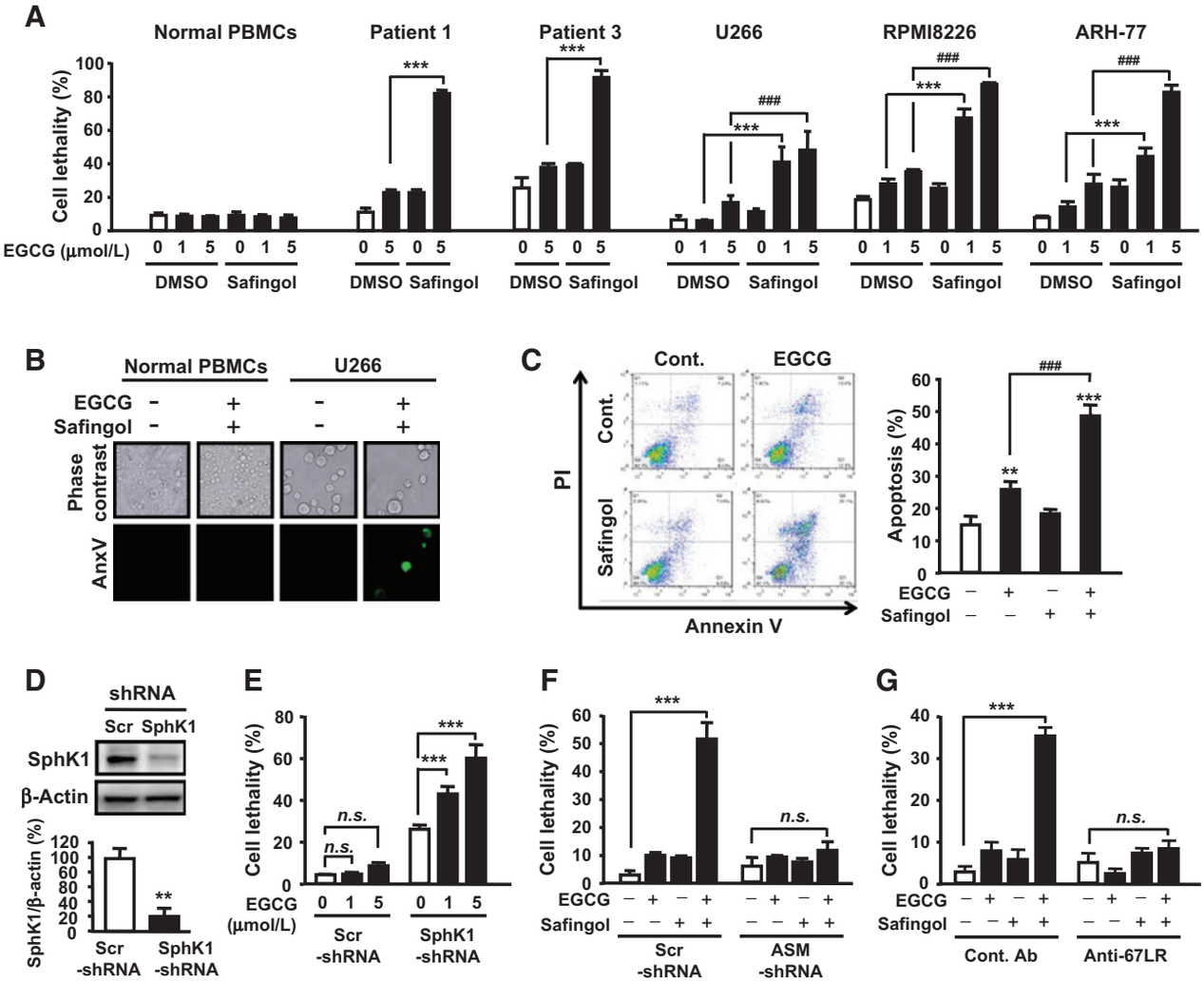

Figure 4.
SphK1 protects cells from 67LR/ASM-dependent apoptotic cell death induced by EGCG. A–C, cells treated with 5 μmol/L EGCG/1 μmol/L safingol for 96 hours were evaluated. Cell viability was evaluated using the trypan blue exclusion method (A). Apoptotic cells were detected by fluorescent microscopy using Annexin V–Alexa Fluor 488 (B). Apoptotic cells were double-stained with Annexin V–Alexa Fluor 488 and PI (C). D and E, effect of silencing SphK1 on EGCG-induced cell death in U266 cells. SphK1 was knocked down by SphK1-specific shRNA in U266 cells (D), and the rate of cell lethality was assessed using the trypan blue exclusion method (E). F, after treatment with 5 μmol/L EGCG and/or 1 μmol/L safingol for 96 hours in SphK1-knockdown U266 cells, the rate of cell lethality was assessed using the trypan blue exclusion method. G, U266 cells were pretreated with either anti-67LR antibodies or control antibodies for 1 hour before stimulation with EGCG (5 μmol/L) and/or safingol (1 μmol/L) for 96 hours, and apoptotic cells were detected using the trypan blue exclusion method. Error bars, SD. $n = 3$ per group. **, $P < 0.01$; *** or ###, $P < 0.001$; n.s., not signficant.

in U266 myeloma cells (Supplementary Fig. S5A and S5B). Furthermore, safingol also has an inhibition activity on PKC. Thus, the effect of PKC on EGCG-induced cell death was confirmed by using a potent inhibitor of PKC Ro-318820. Ro-318820 had no enhancement effect on EGCG-induced cell death either (Supplementary Fig. S6). However, inhibition of SphK1 expression by gene silencing markedly potentiated the anti–multiple myeloma effect of EGCG in U266 cells (Fig. 4D and E). Moreover, U266 cells were protected from EGCG/safingol-induced anti–multiple myeloma activity when ASM protein expression was silenced (Fig. 4F) and when cells were pretreated with anti-67LR antibodies (Fig. 4G). This suggests that the 67LR/ASM pathway is central to cell death induced by combined EGCG/safingol treatment. These results demonstrate that targeting overexpressed 67LR and SphK1 in multiple myeloma cells may be a useful approach for cancer-specific killing.

Combination of EGCG with safingol markedly activates DAPK1 in multiple myeloma cells

A previous study has reported that ceramide activates death-associated protein kinase 1 (DAPK1), a key mediator of apoptosis (28). Therefore, we treated U266 cells with or without EGCG and safingol for 96 hours to identify the effects of combination EGCG/safingol treatment on DAPK1 activity. Treatment with combination EGCG/safingol reduced p-(Ser308)-DAPK1 levels markedly, leading to increased phosphorylation of the DAPK1 substrate myosin regulatory light chain (MRLC), which induces blebbing in apoptotic cells (Fig. 5A and B). Furthermore, DAPK1 was

abnormally elevated in U266 cells compared with normal PBMCs. Treatment of U266 cells with combination EGCG/safingol for 24 hours did not have any effect on p-DAPK1 when cells were pretreated with anti-67LR antibodies or ASM-targeting shRNA (Fig. 5C and D), suggesting that the 67LR/ASM signaling plays a critical role in EGCG/safingol-induced activation of DAPK1.

Combination EGCG/safingol treatment markedly suppresses tumor growth *in vivo*

We evaluated the *in vivo* activity of combination EGCG/safingol on the growth of MPC-11 cell–derived subcutaneous tumors in female BALB/c mice. Combination EGCG/safingol treatment did not affect body weight (Supplementary Fig. S7A) or serum ALT/AST activity (Supplementary Fig. S7B). Treatment with EGCG/safingol markedly suppressed tumor growth in mice (Fig. 6A and B). Moreover, log-rank analysis of Kaplan–Meier survival curves revealed a significant increase in the survival rates of mice treated with combination EGCG/safingol compared with mice exposed to EGCG or safingol alone (Fig. 6C). Finally, tumors from mice treated with combination EGCG/safingol had reduced levels of p-DAPK1 and p-IGF1R (Fig. 6D). These results suggest that cotreatment with safingol increases EGCG-induced antitumor activity in mice.

Discussion

The proliferation and survival of multiple myeloma cells has been linked to the activation of several RTKs [including the ErbB family, HGF-R, platelet-derived growth factor receptor (PDGFR), and IGF1R] and pathways such as PI3K/Akt, JAK/STAT3 mitogen-activated protein kinase (MAPK)/extracellular signal–regulated kinase (ERK), and NF-κB (29–32). Activation of these pathways is dependent on several growth factors, including IL6, IGF1, HGF, heparin-binding EGF-like growth factor, and fibroblast growth factor (33–35) IGF1 decreases drug sensitivity of multiple myeloma cells and upregulates a series of antiapoptotic proteins, including A1/Bfl-1, X chromosome–linked inhibitor of apoptosis (XIAP), and Bcl-2 (36–38). Therefore, modulation of these signaling pathways and/or the signals that initiate them is a potential strategy for cancer therapy.

I-κB kinase (IKK) inhibitors promote multiple myeloma cell apoptosis, and inhibition of IGF1 signaling enhances this effect (39). Therefore, inhibiting IGF1 signaling could enhance the use of IKK inhibitors for multiple myeloma treatment. We have demonstrated that ASM-generated ceramide negatively regulates lipid raft clustering, leading to suppression of RTKs, including IGF1R. Therefore, promoting ASM-generated ceramide production could inhibit IGF1R activation and enhance the effectiveness of IKK inhibitors in multiple myeloma. Moreover, elevated levels of Mer promote proliferation and survival in acute leukemia [acute lymphoblastic leukemia (ALL), AML), breast cancer, astrocytoma, lung cancer, and melanoma (40). Mer silencing increased the sensitivity of ALL cells to a cytotoxic agent *in vitro* and delayed disease onset *in vivo* (41). However, little is known about Mer expression in multiple myeloma cells. We detected aberrant activation of Mer and IGF1R in U266 cells. Because activation of ASM can suppress these receptors,

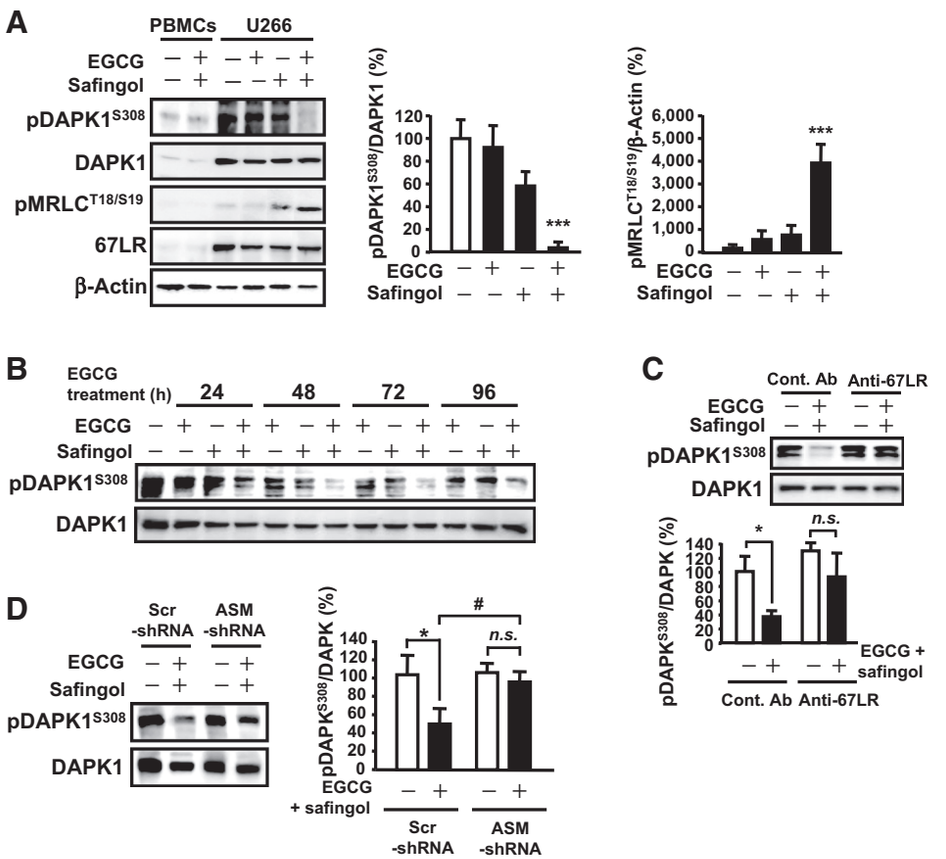

Figure 5.
A combination of EGCG with an SphK1 inhibitor activates DAPK1 in multiple myeloma cells. A, phosphorylation of DAPK1 and MRLC in U266 cells and normal PBMCs after treatment with 5 μmol/L EGCG/1 μmol/L safingol for 96 hours. B, DAPK1 activity in cells treated with 5 μmol/L EGCG/1 μmol/L safingol. C, DAPK1 activity in cells pretreated with anti-67LR/control antibodies and then treated with EGCG/safingol. D, DAPK1 activity in ASM-knockdown U266 cells after treatment with 5 μmol/L EGCG/1 μmol/L safingol. Error bars, SD. $n = 3$ per group. * or #, $P < 0.05$; ***, $P < 0.001$; n.s., not significant.

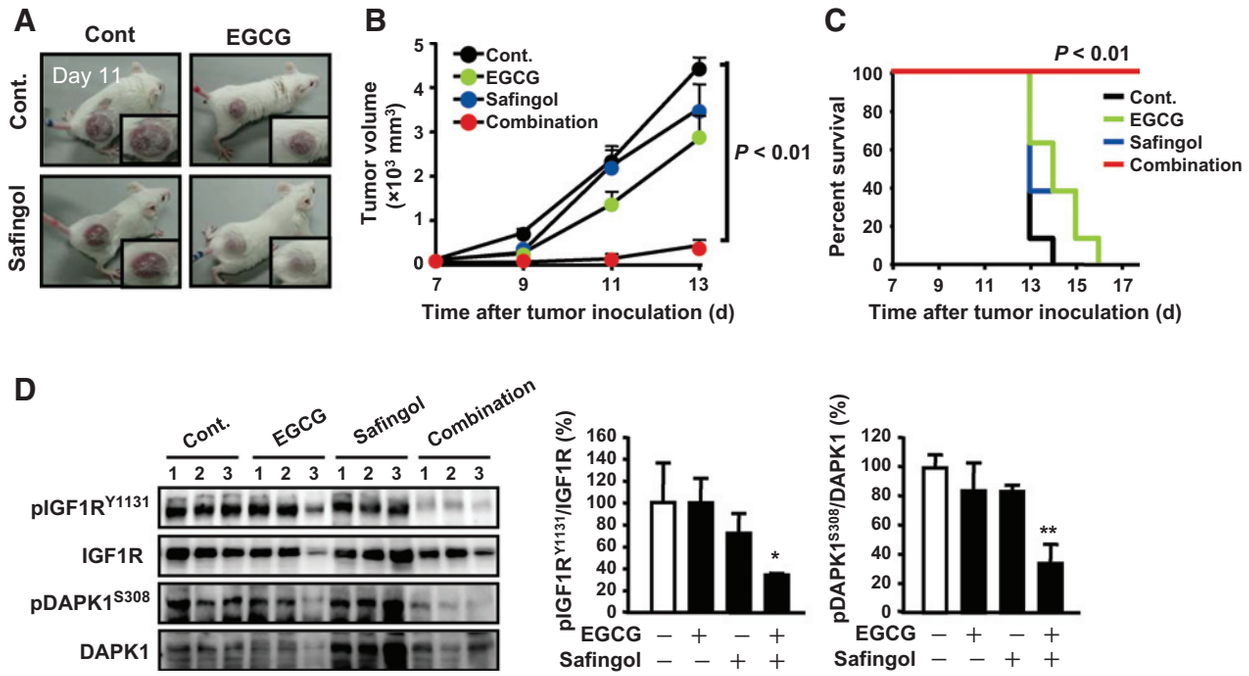

Figure 6.
Combination of EGCG/safingol markedly suppresses tumor growth *in vivo*. A–D, MPC-11 cells were injected subcutaneously into female BALB/c mice, and following the appearance of palpable tumors, the mice were given intraperitoneal injections of EGCG (20 mg/kg) and/or safingol (5 mg/kg). The effects of EGCG alone, safingol alone, or EGCG/safingol combination on flat tumor size (A), tumor growth (B), survival rate (C), and IGF1R and DAPK1 activity in tumor cells (D) were evaluated. Statistical analysis of survival curves was performed using log-rank analysis of the Kaplan–Meier curves. Error bars, SEM. $n = 8$ per group. *, $P < 0.05$; **, $P < 0.01$.

targeting ASM represents a rational approach to multiple myeloma therapy.

IGF1R signaling is impaired by disrupted lipid raft clustering (42). Lipid rafts are plasma membrane microdomains, comprising cholesterol and sphingolipids in ordered domains that control signal transduction, cellular contacts, pathogen recognition, and internalization processes (43). Chemotherapeutic drug-induced ceramide-rich lipid raft clustering triggers activation of death receptors and apoptotic cell death (44). We have discovered that EGCG can disrupt lipid raft formation and suppress IGF1R activation by inducing ceramide accumulation through ASM activation.

EGCG-induced anti-myeloma activities mediated by 67LR are highly specific. However, the concentration of EGCG required to induce sufficient ceramide-rich lipid raft clustering exceeds 10 μmol/L, limiting its therapeutic potential. SphK1 is abnormally elevated in many human cancers, including breast, lung, prostate, and colon cancer (20). We hypothesized that SphK1 may protect multiple myeloma cells from EGCG-induced cell death by down-regulating ceramide levels and upregulating S1P levels. We found that SphK1 was markedly elevated in multiple myeloma cells from both human patients and in multiple myeloma cell lines. We also identified that the SphK1 inhibitor safingol potentiated EGCG-induced lipid raft disruption and IGF1R inhibition, leading to markedly suppressed tumor growth *in vivo*. These results suggest that aberrant expression of SphK1 contributes to EGCG resistance in multiple myeloma cells.

Hepatotoxicity is an adverse effect of high-dose EGCG (45), and elevation of the transaminases ALT and AST has been observed in clinical trials (9). Therefore, our findings hold great clinical value because safingol first entered clinical trials as an anticancer agent, and no adverse toxicity was seen for doses up to 20 mg/kg (23, 46). Importantly, EGCG and safingol in combination did not increase the serum levels of ALT or AST (Supplementary Fig. S4B). Therefore, combination therapy with safingol may enhance the anticancer effects of EGCG.

Interestingly, safingol potentiated EGCG-induced disruption of cholesterol-rich lipid rafts but had no effect on the clustering of ceramide-rich lipid rafts (Supplementary Fig. S2). Recent reports have suggested that ceramide production causes a significant displacement of cholesterol from lipid raft membranes (47, 48). Therefore, safingol-induced suppression of ceramide degradation may trigger the displacement of cholesterol from lipid raft domains, thereby disrupting cholesterol-rich lipid rafts.

DAPK1 is necessary for ceramide-induced cell death in various cell types, and activation of DAPK1 requires dephosphorylation of its Ser308 residue (49). Consistently, we demonstrated that EGCG/safingol in combination caused dephosphorylation of DAPK1 at Ser308 in multiple myeloma cells without having an effect on normal PBMCs. Surprisingly, we found that DAPK1 is abnormally elevated in multiple myeloma cells relative to normal PBMCs. This suggests that activation of DAPK1 could specifically target myeloma cells. Although the mechanism underlying the aberrant expression of DAPK1 in multiple myeloma is unclear, several reports have suggested that DAPK1 plays a role in survival pathways (in addition to its apoptotic role), which are regulated by domains other than Ser308 (49). Therefore, overexpression of DAPK1 may be involved in the progression of multiple myeloma, and additional studies are required to determine why DAPK1 is abnormally elevated in multiple myeloma cells.

We report that EGCG-induced ASM activation triggers RTK inhibition and DAPK1 activation in multiple myeloma cells. Importantly, these effects are mediated by overexpressed 67LR in cancer cells. Moreover, these effects are impaired by aberrant expression of SphK1 in multiple myeloma cells. Inhibition of SphK1 activity by treatment with safingol dramatically potentiates EGCG-induced apoptotic activity both *in vitro* and *in vivo*. Our results suggest that a new strategy of combining an ASM activator with an SphK1 inhibitor could target cancer cells without indiscriminately affecting normal cells, resulting in less toxicity and better tolerability in patients with myeloma.

Disclosure of Potential Conflicts of Interest

T.D. Shanafelt reports receiving a commercial research grant from Polyphenon E International. No potential conflicts of interest were disclosed by the other authors.

Authors' Contributions

Conception and design: S. Tsukamoto, N.E. Kay, T.D. Shanafelt, H. Tachibana
Development of methodology: S. Tsukamoto, Y. Huang, Y. Fujimura, D. Miura, N.E. Kay
Acquisition of data (provided animals, acquired and managed patients, provided facilities, etc.): S. Tsukamoto, Y. Huang, M. Kumazoe, C. Lesnick, S. Yamada, N. Ueda, T. Suzuki, N.E. Kay, H. Tachibana
Analysis and interpretation of data (e.g., statistical analysis, biostatistics, computational analysis): Y. Huang, M. Kumazoe, C. Lesnick, N. Ueda, Y. Fujimura, D. Miura, H. Tachibana
Writing, review, and/or revision of the manuscript: S. Tsukamoto, Y. Huang, M. Kumazoe, N.E. Kay, T.D. Shanafelt, H. Tachibana
Administrative, technical, or material support (i.e., reporting or organizing data, constructing databases): Y. Huang, M. Kumazoe, C. Lesnick, Y. Fujimura, D. Miura
Study supervision: M. Kumazoe, T. Suzuki, S. Yamashita, Y.H. Kim

Acknowledgments

The authors thank Drs. Makoto Ito, Nozomu Okino, Daichi Yukihira (Kyushu University), and Toshiro Okazaki (Kanazawa Medical University) for technical assistance.

Grant Support

This work was kindly supported in part by Grants-in-Aid for Scientific Research (KAKENHI) from the Japan Society for the Promotion of Science to H. Tachibana (grants 22228002 and 15H02448); International Myeloma Foundation (IMF) Japan's grants to H. Tachibana; Research Fellowship for Young Scientists from the Japan Society for the Promotion of Science DC2 (11J01340) to S. Tsukamoto and DC1 (13J03437) to Y. Huang; and MEXT Funding-Project for Developing Innovation Systems-Creation of Innovation Centers for Advanced Interdisciplinary Research Areas Program in Japan to Y. Fujimura and D. Miura.

The costs of publication of this article were defrayed in part by the payment of page charges. This article must therefore be hereby marked *advertisement* in accordance with 18 U.S.C. Section 1734 solely to indicate this fact.

Received March 4, 2015; revised August 6, 2015; accepted August 6, 2015; published OnlineFirst August 11, 2015.

References

1. Kyle RA, Rajkumar SV. Treatment of multiple myeloma: a comprehensive review. Clin Lymphoma Myeloma 2009;9:278–88.
2. Shammas MA, Neri P, Koley H, Batchu RB, Bertheau RC, Munshi V, et al. Specific killing of multiple myeloma cells by (—)-epigallocatechin-3-gallate extracted from green tea: biologic activity and therapeutic implications. Blood 2006;108:2804–10.
3. Britschgi A, Simon HU, Tobler A, Fey MF, Tschan MP. Epigallocatechin-3-gallate induces cell death in acute myeloid leukaemia cells all-transretinoic acid-induced neutrophil differentiation via death-associated protein kinase 2. Br J Haematol 2010;149:55–64.
4. Sanjuan X, Fernandez PL, Miquel R, Munoz J, Castronovo V, Menard S, et al. Overexpression of the 67-kD laminin receptor correlates with tumor progression in human colorectal carcinoma. J Pathol 1996;179:376–80.
5. Viacava P, Naccarato AG, Collecchi P, Menard S, Castronovo V, Bevilacqua G. The spectrum of 67-kD laminin receptor expression in breast carcinoma progression. J Pathol 1997;182:36–44.
6. Scheiman J, Tseng J-C, Zheng Y, Meruelo D. Multiple functions of the 37/67-kd laminin receptor make it a suitable target for novel cancer gene therapy. Mol Ther 2009;18:63–74.
7. Liu L, Sun L, Zhang H, Li Z, Ning X, Shi Y, et al. Hypoxia-mediated up-regulation of MGr1-Ag/37LRP in gastric cancers occurs via hypoxia-inducible-factor 1-dependent mechanism and contributes to drug resistance. J Int Cancer 2009;124:1707–15.
8. Yang CS, Wang X, Lu G, Picinich SC. Cancer prevention by tea: animal studies, molecular mechanisms and human relevance. Nat Rev Cancer 2009;9:429–39.
9. Shanafelt TD, Call TG, Zent CS, LaPlant B, Bowen DA, Roos M, et al. Phase I trial of daily oral polyphenon E in patients with asymptomatic Rai stage 0 to II chronic lymphocytic leukemia. J Clin Oncol 2009;27:3808–14.
10. Bettuzzi S, Brausi M, Rizzi F, Castagnetti G, Peracchia G, Corti A. Chemoprevention of human prostate cancer by oral administration of green tea catechins in volunteers with high-grade prostate intraepithelial neoplasia: a preliminary report from a one-year proof-of-principle study. Cancer Res 2006;66:1234–40.
11. McLarty J, Bigelow RL, Smith M, Elmajian D, Ankem M, Cardelli JA. Tea polyphenols decrease serum levels of prostate-specific antigen, hepatocyte growth factor, and vascular endothelial growth factor in prostate cancer patients and inhibit production of hepatocyte growth factor and vascular endothelial growth factor *in vitro*. Cancer Prev Res 2009;2:673–82.
12. Tachibana H, Koga K, Fujimura Y, Yamada K. A receptor for green tea polyphenol EGCG. Nat Struct Mol Biol 2004;11:380–1.
13. Umeda D, Yano S, Yamada K, Tachibana H. Green tea polyphenol epigallocatechin-3-gallate signaling pathway through 67-kDa laminin receptor. J Biol Chem 2008;283:3050–8.
14. Pollak M. The insulin and insulin-like growth factor receptor family in neoplasia: an update. Nat Rev Cancer 2012;12:159–69.
15. Shimizu M, Deguchi A, Hara Y, Moriwaki H, Weinstein IB. EGCG inhibits activation of the insulin-like growth factor-1 receptor in human colon cancer cells. Biochem Biophys Res Commun 2005;334:947–53.
16. Dimanche-Boitrel MT, Meurette O, Rebillard A, Lacour S. Role of early plasma membrane events in chemotherapy-induced cell death. Drug Resist Updat 2005;8:5–14.
17. Megha, Sawatzki P, Kolter T, Bittman R, London E. Effect of ceramide N-acyl chain and polar headgroup structure on the properties of ordered lipid domains (lipid rafts). Biochim Biophys Acta 2007;1768:2205–12.
18. Casaletto JB, McClatchey AI. Spatial regulation of receptor tyrosine kinases in development and cancer. Nat Rev Cancer 2012;12:387–400.
19. Tsukamoto S, Hirotsu K, Kumazoe M, Goto Y, Sugihara K, Suda T, et al. Green tea polyphenol EGCG induces lipid raft clustering and apoptotic cell death by activating protein kinase C d and acid sphingomyelinase through 67-kDa laminin receptor in multiple myeloma cells. Biochem J 2012; 443:525–34.
20. Vadas M, Xia P, McCaughan G, Gamble J. The role of sphingosine kinase 1 in cancer: oncogene or non-oncogene addition? Biochim Biophys Acta 2008;1781:442–7.
21. Cuvillier O, Ader I, Bouquerel P, Brizuela L, Malavaud B, Mazerolles C, et al. Activation of sphingosine kinase-1 in cancer: implications for therapeutic targeting. Curr Mol Pharmacol 2010;3:53–65.
22. Reynolds CP, Maurer BJ, Kolesnick RN. Ceramide synthesis and metabolism as a target for cancer therapy. Cancer Lett 2004;206:169–80.
23. Schwartz GK, Ward D, Saltz L, Casper ES, Spiess T, Mullen E, et al. A pilot clinical/pharmacological study of the protein kinase C-specific inhibitor safingol alone and in combination with doxorubicin. Clin Cancer Res 1997;3:537–43.

24. Shaner RL, Allegood JC, Park H, Wang E, Kelly S, Haynes CA, et al. Quantitative analysis of sphingolipids for lipidomics using triple quadrupole and quadrupole linear ion trap mass spectrometers. J Lipid Res 2009;50:1692–707.
25. Bielawski J, Szulc ZM, Hannun YA, Bielawska A. Simultaneous quantitative analysis of bioactive sphingolipids by high-performance liquid chromatography-tandem mass spectrometry. Methods 2006;39:82–91.
26. Lee JH, Kishikawa M, Kumazoe M, Yamada K, Tachibana H. Vitamin A enhances antitumor effect of a green tea polyphenol on melanoma by upregulating the polyphenol sensing molecule 67-kDa laminin receptor. PLoS One 2010;5:e11051.
27. Adachi S, Nagao T, Ingolfsson HI, Maxfield FR, Andersen OS, Kopelovich L, et al. The inhibitory effect of (—)-epigallocatechin gallate on activation of the epidermal growth factor receptor is associated with altered lipid order in HT29 colon cancer cells. Cancer Res 2007;67:6493–501.
28. Widau RC, Jin Y, Dixon SA, Wadzinski BE, Gallagher PJ. Protein phosphatase 2A (PP2A) holoenzymes regulate death-associated protein kinase (DAPK) in ceramide-induced anoikis. J Biol Chem 2010;285:13827–38.
29. Hsu J, Shi Y, Krajewski S, Renner S, Fisher M, Reed JC, et al. The AKT kinase is activated in multiple myeloma tumor cells. Blood 2001;98:2853–5.
30. Bereson JR, Ma HM, Vescio R. The role of nuclear factor-kappaB in the biology and treatment of multiple myeloma. Semin Oncol 2001; 28:626–33.
31. Giuliani N, Lunghi P, Morandi F, Colla S, Bonomini S, Hojden M, et al. Downmodulation of ERK protein kinase activity inhibits VEGF secretion by human myeloma cells and myeloma-induced angiogenesis. Leukemia 2004;18:628–35.
32. Catlett-Falcone R, Landowski TH, Oshiro MM, Turkson J, Levitzki A, Savino R, et al. Constitutive activation of Stat3 signaling confers resistance to apoptosis in human U266 myeloma cells. Immunity 1999;10:105–15.
33. Ogata A, Chauhan D, Teoh G, Treon SP, Urashima M, Schlossman RL, et al. IL-6 triggers cell growth via the Ras-dependent mitogen-activated protein kinase cascade. J Immunol 1997;159:2212–21.
34. Frassanito MA, Cusmai A, Iodice G, Dammacco F. Autocrine interleukin-6 production and highly malignant multiple myeloma: relation with resistance to drug-induced apoptosis. Blood 2001;97:483–9.
35. Mahtouk K, Moreaux J, Hose D, Reme T, Meissner T, Jourdan M, et al. Growth factors in multiple myeloma: a comprehensive analysis of their expression in tumor cells and bone marrow environment Affymetrix microarrays. BMC Cancer 2010;10:198–215.
36. Georgii-Hemming P, Wiklund HJ, Ljunggen O, Nilsson K. Insulin-like growth factor I is a growth and survival factor in human multiple myeloma cell lines. Blood 2001;88:2250–8.
37. Pene F, Claessens YE, Muller O, Viguie F, Mayeux P, Dreyfus F, et al. Role of the phosphatidylinositol 3-kinase/Akt and mTOR/P70S6-kinase pathways in the proliferation and apoptosis in multiple myeloma. Oncogene 2002;21:6587–97.
38. Mitsiades CS, Mitsiades N, Poulaki V, Schlossman R, Akiyama M, Chauhan D, et al. Activation of NF-kappaB and upregulation of intracellular anti-apoptotic proteins via the IGF-1/Akt signaling in human multiple myeloma cells: therapeutic implications. Oncogene 2002;21:5673–83.
39. Tagoug I, Sauty De Chalon A, Dumontet C. Inhibition of IGF-1 signalling enhances the apoptotic effect of AS602868, an IKK2 inhibitor, in multiple myeloma cell lines. PLoS One 2011;6:e22641.
40. Verma A, Warner SL, Vankayalapati H, Bearss DJ, Sharma S. Targeting Axl and Mer kinases in cancer. Mol Cancer Ther 2011;10:1763–73.
41. Linger RM, DeRyckere D, Brandao L, Sawczyn KK, Jacobsen KM, Liang X, et al. Mer receptor tyrosine kinase is a novel therapeutic target in pediatric B-cell acute lymphoblastic leukemia. Blood 2009;114:2678–87.
42. Hong S, Huo H, Xu J, Liao K. Insulin-like growth factor-1 receptor signaling in 3T3-L1 adipocyte differentiation requires lipid rafts but not caveolae. Cell Death Differ 2004;11:714–23.
43. Gombos I, Steinbach G, Pomozi I, Balogh A, Vamosi G, Gansen A, et al. Some new faces of membrane microdomains: a complex confocal fluorescence, differential polarization, and FCS imaging study on live immune cells. Cytometry A 2008;73:220–9.
44. Lacour S, Hammann A, Grazide S, Lagadic-Gossmann D, Athias A, Sergent O, et al. Cisplatin-induced CD95 redistribution into membrane lipid rafts of HT29 human colon cancer cells. Cancer Res 2004;64:3593–8.
45. Lambert JD, Kennett MJ, Sang S, Reuhl KR, Ju J, Yang CS. Hepatotoxicity of high oral dose (–)-epigallocatechin-3-gallate in mice. Food Chem Toxicol 2010;48:409–16.
46. Kedderis LB, Bozigian HP, Kleeman JM, Hall RL, Palmer TE, Harrison SD Jr, et al. Toxicity of the protein kinase C inhibitor safingol administered alone and in combination with chemotherapeutic agents. Fundam Appl Toxicol 1995;25:201–17.
47. Megha, London E. Ceramide selectively displaces cholesterol from ordered lipid domains (rafts): implications for lipid raft structure and function. J Biol Chem 2004;279:9997–10004.
48. Ito J, Nagayasu Y, Yokoyama S. Cholesterol-sphingomyelin interaction in membrane and apolipoprotein-mediated cellular cholesterol efflux. J Lipid Res 2000;41:894–904.
49. Stevens C, Lin Y, Harrison B, Burch L, Ridgway RA, Sansom O, et al. Peptide combinatorial libraries identify TSC2 as a death-associated protein kinase (DAPK) death domain-binding protein and reveal a stimulatory role for DAPK in mTORC1 signaling. J Cell Biol 2009;284:334–44.